HHS Public Access

Author manuscript

Sci Signal. Author manuscript; available in PMC 2015 June 05.

Published in final edited form as:

Sci Signal. ; 8(363): ra14. doi:10.1126/scisignal.2005735.

Ski regulates Hippo and TAZ signaling to suppress breast cancer progression

Juliet Rashidian[1], **Erwan Le Scolan**[1], **Xiaodan Ji**[1], **Qingwei Zhu**[1], **Melinda M. Mulvihill**[2], **Daniel Nomura**[2], and **Kunxin Luo**[1,3,*]

[1]Department of Molecular and Cell Biology, University of California, Berkeley, Berkeley, CA 94720, USA

[2]Department of Nutritional Sciences, University of California, Berkeley, Berkeley, CA 94720, USA

[3]Life Sciences Division, Lawrence Berkeley National Laboratory, Berkeley, CA 94720, USA

Abstract

Ski, the transforming protein of the avian Sloan-Kettering retrovirus, inhibits transforming growth factor–β (TGF-β)/Smad signaling and displays both pro-oncogenic and anti-oncogenic activities in human cancer. Inhibition of TGF-β signaling is likely responsible for the pro-oncogenic activity of Ski. We investigated the mechanism(s) underlying the tumor suppressor activity of Ski and found that Ski suppressed the activity of the Hippo signaling effectors TAZ and YAP to inhibit breast cancer progression. TAZ and YAP are transcriptional coactivators that can contribute to cancer by promoting proliferation, tumorigenesis, and cancer stem cell expansion. Hippo signaling activates the the Lats family of kinases, which phosphorylate TAZ and YAP, resulting in cytoplasmic retention and degradation and inhibition of their transcriptional activity. We showed that Ski interacted with multiple components of the Hippo pathway to facilitate activation of Lats2, resulting in increased phosphorylation and subsequent degradation of TAZ. Ski also promoted the degradation of a constitutively active TAZ mutant that is not phosphorylated by Lats, suggesting the existence of a Lats2-independent degradation pathway. Finally, we showed that Ski repressed the transcriptional activity of TAZ by binding to the TAZ partner TEAD and recruiting the transcriptional co-repressor NCoR1 to the TEAD-TAZ complex. Ski effectively reversed transformation and epithelial-to-mesenchyme transition in cultured breast cancer cells and metastasis in TAZ-expressing xenografted tumors. Thus, Ski inhibited the function of TAZ through multiple mechanisms in human cancer cells.

*Corresponding author. kluo@berkeley.edu.

Author contributions: J.R. performed most of the EMT assays as well as biochemical characterization of TAZ regulation by Ski and wrote the draft of the paper; E.L.S. performed luciferase assays and biochemical characterization of Ski-Hippo interaction; X.J. performed soft agar colony assays and in vivo xenograft tumor metastasis assays; Q.Z. performed ubiquitination assays and luciferase assays related to NCoR1; M.M.M. performed mass spectrometric analysis of Ski immunoprecipitates; D.N. performed mass spectrometric analysis and data interpretation; K.L. designed the study, supervised data analysis, and wrote the paper.

Competing interests: The authors declare that they have no competing interests.

SUPPLEMENTARY MATERIALS

www.sciencesignaling.org/cgi/content/full/8/363/ra14/DC1

INTRODUCTION

Ski was initially identified as the transforming protein of the avian Sloan-Kettering retrovirus and induces oncogenic transformation of chicken embryo fibroblasts upon overexpression (1). In agreement with its oncogenic activity, high amounts of Ski have been detected in many human cancer cell lines (2–6). However, beyond its expression profile, the activity of Ski in mammalian cancer appears to be more consistent with a tumor-suppressive role. First, heterozygous Ski knockout mice are more sensitive to chemical-induced carcinogenesis (7). Second, Ski is located at chromosome 1p36, a tumor suppressor locus frequently deleted in melanoma and neuroblastoma (8–10). Finally, reducing Ski abundance in breast and lung cancer cells enhances tumor progression and metastasis in vivo (11). The mechanisms underlying these conflicting observations have not been fully understood.

Ski exerts its biological functions through interaction with various cellular partners, among which the association with the Smad proteins of the TGF-β signaling pathway is the best characterized. Ski interacts with Smads and represses their ability to activate TGF-β responsive genes by disrupting the functional heteromeric Smad complexes, recruiting transcription co-repressor complex, and blocking the binding of transcriptional coactivators to the Smads (12–14). TGF-β signaling suppresses tumor cell proliferation at early stages of tumorigenesis but promotes epithelial-to-mesenchymal transition (EMT), tumor invasion, and metastasis at late malignant stages. The ability of Ski to antagonize TGF-β/Smad may contribute partially to its dual activities in tumorigenesis but may not be the only mechanism underlying the complex roles and regulation of Ski in human cancer.

To uncover additional molecules or pathways regulated by Ski, we identified Hippo signaling components as potential binding partners of Ski. Hippo pathway is an evolutionarily conserved pathway that plays important roles in the regulation of organ size, embryonic development, tumorigenesis, and stem cell self-renewal (15). The core Hippo signaling complex in mammals is composed of two kinases, Mst1 or Mst2 (Mst1/2) and Lats1 or Lats2 (Lats1/2). Mst1/2 forms a complex with the adaptor protein Sav1 to phosphorylate and activate Lats1/2 (16, 17). The activated Lats1/2, in association with the tumor suppressor Mob1, then phosphorylates and inhibits transcriptional coactivators TAZ and YAP (18–22). TAZ and YAP do not directly bind to DNA but can be recruited to their target promoters through binding to the TEAD/TEF transcription factors (21, 23, 24), where they regulate the transcription of genes essential for proliferation, apoptosis, EMT, and breast cancer stemness (20, 21, 25–29). TAZ and YAP can be phosphorylated by Lats1/2 on multiple sites (30). In particular, phosphorylation of TAZ on Ser^{89} (equivalent to Ser^{127} in YAP) allows its binding to 14-3-3, leading to cytoplasm sequestration (18, 19, 21, 31), and phosphorylation on Ser^{311} primes TAZ to be further phosphorylated by CK1e on Ser^{314}, which mediates binding to the F-box–containing E3 ubiquitin ligase β-TrCP, leading to subsequent ubiquitination and degradation of TAZ (32). Thus, the Hippo core kinase complex is an inhibitor of TAZ and YAP.

The activity of the Hippo pathway and TAZ/YAP can be regulated by extracellular diffusible signals and growth factors as well as signals generated through cell-cell junction, tissue architecture, and mechanotransduction (33). These signals include ligands that bind to

various GPCRs [G protein (heterotrimeric guanine nucleotide–binding protein)–coupled receptors] such as lysophosphatidic acid, thrombin, and epinephrine, which stimulate or inhibit nuclear translocation of YAP/TAZ; growth factors such as EGF (epidermal growth factor), IGF (insulin-like growth factor), or Wnt; or signals sensing cell-cell adhesion, junctional structures, polarity, and matrix stiffness. Finally, TAZ also modulates TGF-β signaling through its interaction with various Smad proteins (34–36).

Hippo pathway controls organ size and tumorigenesis in various animal models (19, 37–44). TAZ and YAP are well-established oncogenes (45). In particular, TAZ abundance is increased in invasive breast cancer cell lines and in 20% of breast cancer tissues (46), and high amounts of TAZ correlate with breast tumors of higher histological grade and increased invasiveness as well as increased numbers of cancer stem cells (29). Furthermore, overexpression of TAZ in breast cancer cells, especially the constitutively active TAZS89A, promotes EMT, cancer stem cell expansion, and tumor invasion (29). The *YAP* gene is amplified in various human cancers, and increased YAP protein abundance and nuclear accumulation inversely correlate with disease-free and overall survival of hepatocellular carcinoma patients (45).

Here, we identified Ski as a repressor of TAZ/YAP. We showed that Ski inhibited the transcription activity of TAZ as well as its ability to promote transformation and EMT in mammary epithelial cells through mechanisms both independent of and dependent on the Hippo kinase complex. Our study thus has uncovered a pathway that regulates TAZ/YAP during tumorigenesis.

RESULTS

STK38 is a binding partner for Ski

To identify Ski-associated proteins, we stably expressed Flag-Ski in MCF10A cells. Cellular proteins that bind to Ski were purified by immunoprecipitation with anti-Flag beads from control and Flag-Ski cell lines and analyzed by quantitative MudPIT. Proteins identified by at least five spectral counts and showing a twofold enrichment over the control samples with a P value of <0.05 were selected for further analysis. The serine/threonine kinase 38 (STK38; also known as NDR1) was identified as a Ski-associated protein (table S1). STK38 or NDR1 is a Ser/Thr kinase of the NDR/LATS family that is highly conserved from yeast to human (47). The human NDR/LATS family contains four members: NDR1 (STK38), NDR2 (STK38L), Lats1, and Lats2. We found that Ski not only bound to NDR1 but also bound strongly to Lats2 and weakly to NDR2. It did not bind to Lats1 (Fig. 1A). These interactions were specific because immunoprecipitation with anti-Flag in cells expressing Flag-Ski alone, hemagglutinin (HA)–HDR1 alone, or Myc-Lats2 alone did not yield associated proteins (Fig. 1A and fig. S1, A and B). Thus, Ski strongly interacts with at least two members of the NDR family. Because the regulation and functions of NDR1 and NDR2 are not well understood, we decided to focus on the interaction of Ski with Lats2 in this study.

Ski interacts with multiple components of the Hippo pathway

Because Lats2 is a part of the core Hippo kinase complex and Lats proteins regulate TAZ and YAP (15), we next investigated whether Ski also associated with other members of the Hippo pathway by coimmunoprecipitation assays. In addition to Lats2, Ski bound to several members of the Hippo pathway including Sav, Mob, and Mer, but not to Mst2, Lats1, YAP, or TAZ (Fig. 1B), suggesting that the physical interactions between Ski and the Hippo pathway members are selective. Again, the interactions were specific because associated proteins were not detected in anti-Flag immunoprecipitates from cells expressing Flag-Ski alone (Fig. 1B) or a bait protein alone (such as HA-Mer, fig. S1C). In addition, endogenous Ski associated with endogenous Lats2, Mer, Sav, and Mob, but not Mst2, in a coimmunoprecipitation assay in MDA-MB-231 breast cancer cells that have relatively high amounts of Ski (Fig. 1C). These interactions were not detected in cells with Ski knockdown (11) (Fig. 1C). Together, our data show that Ski specifically interacted with multiple components of the core Hippo pathway.

Ski inhibits the transcription activity of TAZ/YAP

TAZ and YAP are critical downstream effectors of the Hippo pathway. In the absence of Hippo signaling, they bind to the TEAD DNA binding transcription factor and activate transcription of various genes. The activities of TAZ and YAP are inhibited by the Hippo core kinase complex through phosphorylation (19, 21). Given that Ski interacts with multiple Hippo pathway components, we wondered if it would affect the transcriptional activity of TAZ and YAP. In a luciferase reporter assay, Ski inhibited the transcription activity of TAZ (Fig. 1D) and YAP (Fig. 1E) to a similar extent as did Lats2, whereas reducing endogenous Ski with a short hairpin RNA (shRNA) or two small interfering RNA (siRNA) pools increased the transcription activity of both transfected and endogenous TAZ (Fig. 1, F and G, and fig. S1, D and E). Ski not only inhibited TAZ transcription in the luciferase assay but also, when overexpressed, decreased the abundance of endogenous CTGF (Fig. 1H), which is encoded by a TAZ target gene (48). Thus, Ski inhibited TAZ and YAP transcriptional activity.

The ability of Ski to interact with the Hippo pathway components and inhibit TAZ or YAP is independent of its ability to antagonize TGF-β/Smad signaling. Mutant Ski defective in binding to Smad2/3 (Ski4A16) or Smad4 (SkiW274E) or both (mSki) readily associated with Lats2, Mer, Sav, and Mob and inhibited transcriptional activation induced by TAZ (fig. S2, A to C). Thus, Ski likely promoted Hippo pathway and inhibited TAZ/YAP activation by directly acting on the Hippo pathway.

Ski antagonizes TAZ-induced transformation and EMT

As previously reported, stable overexpression of TAZ in human MCF10A mammary epithelial cells induced anchorage-independent growth and EMT (Fig. 2) (21, 46). Because Ski inhibited TAZ and YAP transcription activities, we investigated whether it could reverse TAZ-induced cell transformation and EMT. We tested MCF10A/TAZ cell lines that stably overexpressed either a Ski complementary DNA (cDNA) or shRNAs targeting Ski (Fig. 2A) in various transformation and EMT assays. Overexpression of Ski significantly blocked TAZ-induced anchorage-independent growth (Fig. 2B). When cultured in the three-

dimensional (3D) Matrigel, MCF10A cells undergo morphological differentiation to form a polarized, multicellular acinus-like structure. Overexpression of TAZ increased the size of the acini (Fig. 2C) as reported previously (21, 49). Overexpression of Ski markedly reduced the size of acini formed by the TAZ-expressing cells back to that of the control acini, and Ski knockdown further increased the size of TAZ-acini (Fig. 2C). Consistently, reducing Ski alone in MCF10A cells caused a moderate increase in acinar size, an increase that was reversed by TAZ knockdown (Fig. 2C and fig. S3A). These large acini had similar polarity and structural organization to those derived from control cells (fig. S3B). Overexpression of Ski also reversed multiple EMT processes induced by TAZ, including actin stress fiber formation (Fig. 2D), increased cell motility (Fig. 2E), decrease in E-cadherin abundance, and increase in vimentin abundance (Fig. 2F). Conversely, reducing Ski in TAZ-expressing cells further enhanced these processes (Fig. 2, D and E). Two additional clones expressing Ski shRNA (fig. S3, A, C, and D) as well as another Ski shRNA clone overexpressing TAZ (fig. S3D) showed similar changes in acinar size and/or cell motility. Together, our data suggest that Ski antagonized the biological activities of TAZ.

Ski enhances the phosphorylation of TAZ/YAP by Lats2

Given that phosphorylation of TAZ and YAP by Lats1/2 inhibits their biological activities, we next asked whether Ski inhibited TAZ and YAP by increasing their phosphorylation by Lats2 using an in vitro kinase assay. Myc immunoprecipitates from 293T cells expressing Myc-Lats2 together with or without Mst2 and/or Ski were subjected to in vitro kinase assays using bacterially purified glutathione *S*-transferase (GST)–TAZ or GST-YAP as exogenous substrates. Lats2 phosphorylated TAZ or YAP (Fig. 3A and fig. S4A), and this phosphorylation was enhanced by the coexpression of Mst2, as expected (16, 17, 19, 21, 22). Ski alone had a modest effect on the activity of Lats2, but in the presence of Mst2, Ski markedly increased the phosphorylation of TAZ/YAP (Fig. 3A and fig. S4A), suggesting that Ski may promote the activation of Lats2.

To further confirm the stimulatory effect of Ski on the kinase activity of Lats2, endogenous Lats2 was isolated from control or MCF10A cells stably expressing Ski or Ski shRNA and subjected to in vitro kinase assays with GST-TAZ as an exogenous substrate. Indeed, Lats2 from Ski-expressing cells showed significantly increased kinase activity, whereas that from cells with Ski knockdown displayed slightly reduced activity, due possibly to the low amount of endogenous Ski in the MCF10A cells (Fig. 3B). Autophosphorylation of Lats2 was also increased in Ski-expressing cells (Fig. 3B).

Phosphorylation of TAZ may lead to its degradation in a ubiquitination-and proteasome-dependent manner or alter its intracellular localization (50). We found that Ski did not affect the localization of TAZ (fig. S4B) but promoted its polyubiquitination (fig. S4C) and shortened its half-life as shown by a pulse-chase assay (Fig. 3C). Consistent with this observation, the abundance of endogenous TAZ was substantially higher in cells with Ski knockdown (Fig. 3D) and lower in cells overexpressing Ski (Fig. 3E). Thus, Ski enhanced the kinase activity of Lats2 and subsequently its phosphorylation of TAZ, leading to its degradation.

Ski facilitates the formation of the core Hippo kinase complex

Activation of Lats2 requires the kinase Mst2 as well as the accessory molecules Sav and Mob. Sav binds to Mst2 and facilitates its interaction with Lats2 and Mob. Because Ski also interacts with Sav and Mob, we hypothesized that Ski could facilitate activation of Lats2 by strengthening the Hippo kinase complex. Indeed, Ski overexpression induced a corresponding increase in the binding of Sav to Lats2 (Fig. 3F). In contrast, Ski had no apparent effect on the abundance of Sav and Mst2 (Fig. 3F and fig. S4D). Thus, Ski likely enhanced Lats2 activation by facilitating its interaction with Mst2 through Sav.

If Ski inhibition of TAZ indeed requires Lats2, Lats2 knockdown in cells expressing Ski and TAZ would be expected to block the Ski inhibition and restore the transcription and transforming activity of cells to that found in cells expressing TAZ alone. Indeed, Lats2 knockdown into the TAZ+Ski cells restored acinar size in the 3D assay (Fig. 3G) and actin stress fiber formation (Fig. 3H). Consistent with these findings, overexpression of Lats2 in cells with Ski knockdown reduced acini size (fig. S4E) and cell motility (fig. S4F). These results indicate that Lats2 is critical for Ski-mediated inhibition of TAZ, at least to some extent.

Similarly, if Sav is absolutely necessary for Ski activation of Lats2, deleting Sav might block the inhibition of TAZ by Ski. Surprisingly, however, in ACHN cells that lack a functional Sav gene, overexpression of Ski still inhibited TAZ transcription (Fig. 4A). This finding suggests that in addition to inhibiting TAZ by activating Lats2 (Lats2-dependent mechanism), Ski could also suppress TAZ at a step downstream of Lats2 activation (Lats2-independent mechanism). Furthermore, although reducing Lats2 abundance by two different siRNAs restored the ability of cells expressing TAZ and Ski to support transcription to a similar extent as cells expressing TAZ alone (Fig. 4B and fig. S4G), Ski still inhibited TAZ in cells with Lats2 knockdown, again supporting the existence of a Lats2-independent mechanism of TAZ repression.

Ski can also inhibit TAZ signaling independently of Lats2-mediated phosphorylation

To further test whether Ski could also inhibit TAZ through a Lats2-independent mechanism, we used the TAZS89A mutant that cannot be phosphorylated by Lats2 and found that Ski inhibited transcriptional activation induced not only by wild-type TAZ but also by TAZS89A (Fig. 4C). We also investigated whether Ski could reverse the transforming phenotypes induced by TAZS89A. In MCF10A cells stably expressing TAZS89A (Fig. 4D), ectopic expression of Ski rescued some, but not all, of the transforming phenotypes induced by the TAZS89A mutant. When cultured in 3D Matrigel, whereas cells expressing TAZS89A were highly transformed and formed disorganized and irregular colonies with fully disrupted apicalbasal polarity, introduction of Ski effectively restored organized epithelial structure and polarity of the acini as indicated by the increased abundance of α_6-integrin on the basolateral side of the acini (Fig. 4E). Although the rescue of 3D morphogenesis by Ski was not complete because the acini were still larger than control MCF10A acini, Ski nevertheless substantially reduced the transforming activity of TAZS89A in MCF10A cells. Consistent with this, Ski impaired anchorage-independent growth of TAZS89A-expressing cells (Fig. 4F). In addition to inhibiting cell transformation,

Ski also partially inhibited stress fiber formation (Fig. 4G), increased E-cadherin abundance, and suppressed vimentin abundance (Fig. 4H). Although Ski partially increased the motility of TAZS89A-expressing cells, the difference was not statistically significant (Fig. 4I). Finally, as a first step in determining whether Ski can inhibit the ability of TAZS89A to promote breast cancer metastasis in vivo, we intravenously injected MCF10A cells expressing TAZS89A alone or with Ski into nude mice, and examined lung metastasis 12 weeks later. Histological analyses revealed a significant decrease in the number of metastatic lesions produced by Ski-coexpressing cells (Fig. 4J). Consistent with this finding, we have previously shown that depletion of Ski enhances the metastasis of breast cancer cells to the bone and lung in a xenograft model (11). Evaluation of the activation state of TAZ and whether knockdown of TAZ can reverse the effects of Ski depletion on the enhanced metastasis in this xenograft assay will more clearly show that Ski can inhibit breast cancer progression through TAZ in vivo. Nonetheless, these results indicate that Ski could suppress TAZ through both Lats2-dependent and Lats2-independent mechanisms.

Ski also induces degradation of TAZS89A in a Lats-independent manner

We next used the pulse-chase assay and found that Ski markedly reduced the half-life of TAZS89A (Fig. 5A). Consistent with this finding, the amount of TAZS89A was lower in cells overexpressing Ski (Fig. 5B). In addition, the abundance of another TAZ mutant, S311A, which is also defective in Lats1/2 phosphorylation (32), was similarly reduced in cells overexpressing Ski (Fig. 5C). Finally, the proteasome inhibitor *N*-carbobenzyloxy-L-leucyl-L-leucyl-L-leucinal (MG132) stabilized Ski-induced degradation of both wild-type TAZ and TAZS89A (Fig. 5D), suggesting that this degradation event requires the proteasome. Although the stem cell factor (SCF)/CRL1$^{\beta\text{-TrCP}}$ E3 ligase (β-TrCP) has been reported to mediate TAZ degradation triggered by Lats-mediated phosphorylation (32), knocking down β-TrCP with siRNA did not block TAZ degradation by Ski (fig. S5), indicating that Ski-induced TAZ degradation is not mediated by the β-TrCP E3 ligase. Thus, in addition to promoting Lats2-dependent phosphorylation and degradation of TAZ, Ski can also induce TAZ degradation through a Lats2-independent mechanism. The identity of the E3 ubiquitin ligase that mediates Ski-induced and Lats-independent TAZ degradation will be determined in future studies.

Ski directly represses TAZ transcription by recruiting NCoR1

Finally, because TAZ activates transcription through binding to its DNA binding partner TEAD and possibly other transcription coactivators (27), we asked whether Ski could repress TAZ transcription by blocking its interaction with TEAD and/or by recruiting a transcription co-repressor to its target promoter. In a coimmunoprecipitation assay, endogenous Ski bound to endogenous TEAD (Fig. 6A), but this binding did not appear to affect the TAZ-TEAD interaction (Fig. 6B). Because Ski can bind to the transcriptional co-repressor NCoR1 (12, 51), we next asked whether Ski could recruit NCoR1 to the TEAD/TAZ complex through its association with TEAD to repress TAZ activity. Indeed, whereas TEAD did not bind to NCoR1 in the absence of Ski, it formed a complex with NCoR1 when Ski was expressed (Fig. 6C). The interaction between endogenous TEAD and NCoR1 could also be detected in cells that stably express Ski at amounts similar to those found in malignant cancer cells (Fig. 6D). Over-expression of NCoR1 repressed the

transcriptional activity of TAZ (Fig. 6E), an effect that required Ski (Fig. 6E). These findings are consistent with a model in which Ski recruits NCoR1 to repress TAZ transcription activity. Finally, NCoR1 knockdown partially impaired the ability of overexpressed Ski to inhibit TAZ (Fig. 6E), confirming that Ski could repress TAZ in an NCoR1-dependent manner, but also suggesting that NCoR1-independent mechanisms also played a role in Ski-mediated inhibition of TAZ. Thus, Ski might directly inhibit TAZ transcription by recruiting transcriptional co-repressors to TAZ through binding to TEAD, and this could be a Lats2-independent mechanism of TAZ inhibition by Ski.

DISCUSSION

TAZ is a critical effector of the Hippo pathway and plays an essential role in breast cancer progression because high amounts of TAZ can promote tumor growth, EMT, and breast cancer stem cell expansion (15, 29). Here, we identified Ski as a novel inhibitor of TAZ signaling in breast cancer cells by facilitating its degradation through both Lats2-dependent and Lats2-independent mechanisms and by directly repressing the transcriptional activity of TAZ. Ski bound to multiple components of the Hippo core kinase complex to enhance the kinase activity of Lats2, leading to increased phosphorylation of TAZ and subsequent degradation. In this capacity, it may function as a scaffolding protein to increase the affinity of Mst and Sav for Lats2 to facilitate its activation. In addition, Ski could directly promote TAZ degradation in a Lats2-independent manner through recruiting a yet to be identified E3 ubiquitin ligase to TAZ. Finally, Ski also recruited the transcriptional co-repressor NCoR1 to the TEAD/TAZ complex to inhibit TAZ transcriptional activity. Thus, Ski could serve as a potent inhibitor of TAZ by promoting its degradation or suppressing its transcriptional activity through multiple mechanisms, and thus in this capacity functions as a strong antitumorigenic barrier against the malignant progression of breast cancer cells. Inactivation of this regulation by reducing Ski abundance or by disrupting the interaction between Ski and its partners may be a critical step in breast cancer progression. Indeed, Ski not only inhibited TAZ-dependent transcription activation but also effectively reversed TAZ-induced transformation, EMT, and metastasis of breast cancer cells. Thus, Ski regulates Hippo signaling and inhibits the oncogenic TAZ protein in human cancer cell lines.

Ski contains both pro-oncogenic and anti-oncogenic activities in mammalian cells (52), and its pro-oncogenic activity is related to its ability to antagonize the tumor suppressor activity of TGF-β/Smads at early stage of tumor development (53). In late stages of malignant cancers, the TGF-β/Smad pathway switches from tumor suppression to tumor promotion by inducing various aspects of EMT, invasion, and changes in the micro-environment (54). At this point, Ski could suppress the tumor-promoting activity of TGF-β/Smad (55). Our work reported here has revealed another important mechanism by which Ski exerts its antitumorigenic activity by repressing the ability of TAZ to promote EMT and metastasis in breast cancer cells. Thus, Ski is pro-oncogenic at early stages of tumorigenesis but functions as a tumor suppressor at later stages of tumor progression by inhibiting the tumor-promoting activities of TAZ/YAP.

Our study has shown that Ski could inhibit TAZ function through both Lats2-dependent and Lats2-independent pathways. The importance of the Lats2-dependent pathway is

demonstrated by a number of experiments using a combination of Lats2 knockdown or overexpression strategies, and the ability of Ski to antagonize various activities induced by the TAZS89A mutant that is refractory to Lats2 inhibition strongly supported the functional importance of a Lats2-independent model. At this time, it is difficult to evaluate the relative contributions of the two mechanisms in Ski regulation of TAZ signaling. In any given cell, the mechanism that is in operation likely depends on the physiological context (cell types, developmental stages, or microenvironment) and the presence of other signaling pathways. Given that both TAZ and Ski are highly abundant in malignant cancer cells or normal cells at a specific developmental stage, these cell types are likely the ones in which this regulation will occur.

Several E3 ubiquitin ligases have been linked to the regulation of TAZ stability. Apart from the destruction complex [APC (adenomatous polyposis coli)/Axin/GSK-3 (glycogen synthase kinase-3)] in the Wnt pathway that facilitates TAZ degradation together with β-catenin (56), $SCF^{\beta\text{-}TrCP}$ binds to TAZ that has been phosphorylated by both Lats2 and CK1ε and targets it for ubiquitination and degradation (32). The Hect domain E3 ligase ITCH (also known as AIP4) can also be recruited to YAP by AMOT to promote YAP ubiquitination and degradation (57). In our study, β-TrCP knockdown did not result in the stabilization of TAZ, suggesting that a yet to be identified E3 ligase may mediate Ski-induced TAZ degradation. This notion opens new doors for future investigations.

Upstream factors or pathways that regulate Ski abundance during development or cancer have not been well defined. TGF-β decreases Ski abundance in malignant melanoma and breast cancer cells through the E3 ligase Arkadia, which is recruited to Ski by the R-Smad proteins to promote its degradation (11). This suppression of Ski by TGF-β may provide a mechanism by which TGF-β could coordinate with the TAZ/YAP pathway to promote tumor progression in malignant cancer cells. Thus, in addition to the Hippo pathway, mechanical cues, ECM stiffness, cytoskeleton tension, cell shape change, Wnt signaling, and GPCR-Rho signaling (15), the abundance and activity of TAZ and YAP can also be regulated by TGF-β signaling through Ski.

In summary, our study showed that Ski abrogated the activity of TAZ through multiple mechanisms in human mammary epithelial cells, has established Ski as an important tumor suppressor in breast cancer, and has also identified a regulator of the Hippo pathway as well as a new point of crosstalk between TGF-β and Hippo signaling.

MATERIALS AND METHODS

Cell culture, antibodies, siRNAs, and transfection

293T and HEK293 cells were cultured in Dulbecco's modified Eagle's medium (DMEM) supplemented with 10% fetal bovine serum (FBS), penicillin (100 U/ml), and streptomycin (all from Invitrogen). MCF10A cells were maintained in DMEM/F-12 medium supplemented with 5% horse serum, EGF (20 ng/ml), hydrocortisone (0.5 μg/ml), insulin (10 μg/ml), cholera toxin (100 ng/ml), and penicillin and streptomycin. Antibodies specific for the following proteins were used at the indicated concentrations: Ski (1:1000, G8, Cascade Bioscience); Flag (1:5000, Sigma); HA (1:2000, Sigma); Myc (1:5000, 9E10,

Roche Diagnostics); Lats2 (1:1000, Bethyl Laboratories); Mst2 (1:1000, Cell Signaling); Mer, Sav, Mob, YAP, and CTGF (all 1:1000, Santa Cruz Biotechnology); TEAD1 (1:1000, BD Transduction Laboratories); TAZ (1:1000, BD Pharmingen); E-cadherin (1:1000 for Western blotting and 1:400 for immunostaining, Cell Signaling); vimentin (1:1000, BD Transduction Laboratories); MAB 1378 (anti–α_6-integrin; 1:200, Chemicon); GM130 (Golgi matrix marker; 1:200, BD Biosciences); β-TrCP (1:1000, Cell Signaling); NCoR1 (1:1000, Santa Cruz Biotechnology); and tubulin (1:3000, EMD Millipore). Rhodamine-phalloidin was used for actin fiber staining (1:80, Life Technologies).

The following siRNAs from Dharmacon were used: siGENOME Human LATS2 (26524) siRNA SMARTpool (#M-003865-02-0002); Accell Human SKI (6497) siRNA Set of 4 Upgrade (EU-003927-00-0002); Accell Human SKI (6497) siRNA SMARTpool (E-003927-00-0005); Accell Non-targeting siRNA pool (D-001910-10-05); siGENOME β-TrCP siRNA SMARTpool (M-003463-01-0005), Set of 4 Upgrade; Accell WWTR1 siRNA (TAZ siRNA). The following siRNAs from Qiagen were used: Hs-LATS2-7 FlexiTube siRNA (SI02660154), AllStars Negative Control siRNA (1027281). We obtained the NCoR1 siRNA (h) (sc-36001) from Santa Cruz Biotechnology. The sequence within human Ski cDNA targeted by the shRNA oligonucleotide pair was 5′-GTACTCGGCCCAGATCGAA-3′.

Transfection and infection

All cDNA transfections were performed using the Lipofectamine Plus transfection system (Invitrogen). siRNAs were transfected using Lipofectamine RNAiMAX (Invitrogen). Stable MCF10A cells lines were generated through retroviral infection as described previously by Zhu *et al*. (55).

Luciferase assay

To measure TAZ/YAP transcriptional activity, HEK293 or 293T cells were transfected with either an 8×GT-IIC Luciferase reporter (25) and the indicated cDNAs or siRNAs. Thirsty-six hours after transfection, cells were lysed and luciferase activity was measured.

Immunoprecipitation and Western blotting

Cells were lysed in high- or low-salt lysis buffer [150 to 400 mM NaCl, 50 mM Hepes-KOH (pH 7.8), 5 mM EDTA, 1% NP-40, 3 mM dithiothreitol, 0.5 mM phenylmethylsulfonyl fluoride, aprotinin (10 μg/ml)], and cell lysates were precleared with protein A Sepharose for 30 min at 4°C. Precleared lysates were then subjected to immunoprecipitation with the appropriate antibodies as described previously (55). Endogenous Hippo signaling proteins were immunoprecipitated with antibodies against Lats2, Mst2, Mer, Sav, Mob, and TEAD4, and the associated Ski was examined by Western blotting with anti-Ski.

In vitro kinase assay

Lats2 was isolated from cells by immunoprecipitation with anti-Lats2 and incubated with 3 to 4 μg of GST-TAZ or GST-YAP and 5 μCi of [γ-^{32}P]adenosine triphosphate (3000 Ci/mmol) at 30°C for 30 min as previously described (20).

3D culture

Differentiation of MCF10A cells in the 3D Matrigel was performed as previously described (58). After 6 days in the 3D culture, morphological differentiation was examined by phase-contrast microscopy and by immunofluorescence staining for α_6-integrin and GM130 as markers of basal lateral and apical polarity, respectively. Microscopy was performed on a Zeiss LSM710 confocal microscope at the Berkeley Biological Imaging Facility. The localization of the markers was viewed in serial confocal cross-sections.

EMT assays

To assess actin stress fiber staining, cells on coverslips were fixed in 4% paraformaldehyde for 20 min and permeabilized in 0.1% Triton X-100, and actin filaments were stained with rhodamine-phalloidin for 30 min at room temperature as described previously (55). In the wound healing assay, cells were cultured in six-well plates until they reached 90 to 100% confluency. One-milliliter plastic tips were used to generate wounds across the wells. Phase-contrast pictures were taken at the time of wounding (0 hours) and 18 hours later. The wound size was measured at 18 hours, normalized to the 0-hour measurements, and plotted. Experiments were repeated at least three times. E-cadherin and vimentin abundance was examined by Western blotting after the cells reached confluency.

Soft agar assay

Cells were seeded in 0.375% top agar in growth medium over a layer of 0.6% agar in a six-well plate at a density of 4×10^3 cells per well. After 4 weeks of incubation, colonies were stained with MTT and counted.

Pulse-chase assay

Cells in 60-mm dishes were incubated in methionine-free DMEM plus 10% dialyzed FBS for 20 min and pulse-labeled with 300 μCi of [^{35}S]methionine in the same medium for 30 min. The cells were then chased with complete medium as described previously (59).

In vivo metastasis assay

To evaluate the metastasis potential of breast cancer cells, 2×10^6 cells in 150 μl of serum-free medium were injected into the tail veins of 6-week-old female nude mice. After 12 weeks, mice were sacrificed, and quantitation of metastatic colonies was performed on representative H&E-stained sections of formalin-fixed and paraffin-embedded lungs as described previously (60).

In vitro ubiquitination assay

293T cells were transfected with histidine-tagged ubiquitin together with HA-TAZ, Flag-Ski, Flag-Lats2, and Flag-Mst2. Ubiquitinated proteins in the cell lysates were pulled down with Ni^{2+}-NTA beads, and ubiquitinated TAZ was detected by Western blotting with anti-TAZ antibody.

Supplementary Material

Refer to Web version on PubMed Central for supplementary material.

Acknowledgments

We thank K.-L. Guan and A. Mauviel for providing cDNAs of components of Hippo pathway, B. West for the NCoR1 cDNA, and E. Purdom for assistance in reviewing the methods used in statistical analysis. We are grateful to A. Mauviel and Q. Zhu for helpful discussions.

Funding: This work is supported by NIH RO1 CA101891, R21 CA187632, and RO1 DK090347 to K.L. and Susan G. Komen for the Cure KG101263 to J.R.

REFERENCES AND NOTES

1. Li Y, Turck CM, Teumer JK, Stavnezer E. Unique sequence, *ski*, in Sloan-Kettering avian retroviruses with properties of a new cell-derived oncogene. J Virol. 1986; 57:1065–1072. [PubMed: 3754014]
2. Reed JA, Bales E, Xu W, Okan NA, Bandyopadhyay D, Medrano EE. Cytoplasmic localization of the oncogenic protein Ski in human cutaneous melanomas in vivo: Functional implications for transforming growth factor β signaling. Cancer Res. 2001; 61:8074–8078. [PubMed: 11719430]
3. Fukuchi M, Nakajima M, Fukai Y, Miyazaki T, Masuda N, Sohda M, Manda R, Tsukada K, Kato H, Kuwano H. Increased expression of c-Ski as a co-repressor in transforming growth factor-β signaling correlates with progression of esophageal squamous cell carcinoma. Int J Cancer. 2004; 108:818–824. [PubMed: 14712482]
4. Buess M, Terracciano L, Reuter J, Ballabeni P, Boulay JL, Laffer U, Metzger U, Herrmann R, Rochlitz C. Amplification of SKI is a prognostic marker in early colorectal cancer. Neoplasia. 2004; 6:207–212. [PubMed: 15153332]
5. Heider TR, Lyman S, Schoonhoven R, Behrns KE. Ski promotes tumor growth through abrogation of transforming growth factor-β signaling in pancreatic cancer. Ann Surg. 2007; 246:61–68. [PubMed: 17592292]
6. Ritter M, Kattmann D, Teichler S, Hartmann O, Samuelsson MK, Burchert A, Bach JP, Kim TD, Berwanger B, Thiede C, Jager R, Ehninger G, Schafer H, Ueki N, Hayman MJ, Eilers M, Neubauer A. Inhibition of retinoic acid receptor signaling by Ski in acute myeloid leukemia. Leukemia. 2006; 20:437–443. [PubMed: 16424870]
7. Shinagawa T, Nomura T, Colmenares C, Ohira M, Nakagawara A, Ishii S. Increased susceptibility to tumorigenesis of *ski*-deficient heterozygous mice. Oncogene. 2001; 20:8100–8108. [PubMed: 11781823]
8. Smedley D, Sidhar S, Birdsall S, Bennett D, Herlyn M, Cooper C, Shipley J. Characterization of chromosome 1 abnormalities in malignant melanomas. Genes Chromosomes Cancer. 2000; 28:121–125. [PubMed: 10738310]
9. Colmenares C, Heilstedt HA, Shaffer LG, Schwartz S, Berk M, Murray JC, Stavnezer E. Loss of the *SKI* proto-oncogene in individuals affected with 1p36 deletion syndrome is predicted by strain-dependent defects in $Ski^{-/-}$ mice. Nat Genet. 2002; 30:106–109. [PubMed: 11731796]
10. Brodeur GM. Neuroblastoma: Biological insights into a clinical enigma. Nat Rev Cancer. 2003; 3:203–216. [PubMed: 12612655]
11. Le Scolan E, Zhu Q, Wang L, Bandyopadhyay A, Javelaud D, Mauviel A, Sun L, Luo K. Transforming growth factor-β suppresses the ability of Ski to inhibit tumor metastasis by inducing its degradation. Cancer Res. 2008; 68:3277–3285. [PubMed: 18451154]
12. Luo K, Stroschein SL, Wang W, Chen D, Martens E, Zhou S, Zhou Q. The Ski oncoprotein interacts with the Smad proteins to repress TGFβ signaling. Genes Dev. 1999; 13:2196–2206. [PubMed: 10485843]
13. Akiyoshi S, Inoue H, Hanai J, Kusanagi K, Nemoto N, Miyazono K, Kawabata M. c-Ski acts as a transcriptional co-repressor in transforming growth factor-β signaling through interaction with smads. J Biol Chem. 1999; 274:35269–35277. [PubMed: 10575014]

14. Wu JW, Krawitz AR, Chai J, Li W, Zhang F, Luo K, Shi Y. Structural mechanism of Smad4 recognition by the nuclear oncoprotein Ski: Insights on Ski-mediated repression of TGF-β signaling. Cell. 2002; 111:357–367. [PubMed: 12419246]
15. Yu FX, Guan KL. The Hippo pathway: Regulators and regulations. Genes Dev. 2013; 27:355–371. [PubMed: 23431053]
16. Chan EH, Nousiainen M, Chalamalasetty RB, Schafer A, Nigg EA, Sillje HH. The Ste20-like kinase Mst2 activates the human large tumor suppressor kinase Lats1. Oncogene. 2005; 24:2076–2086. [PubMed: 15688006]
17. Praskova M, Xia F, Avruch J. MOBKL1A/MOBKL1B phosphorylation by MST1 and MST2 inhibits cell proliferation. Curr Biol. 2008; 18:311–321. [PubMed: 18328708]
18. Hao Y, Chun A, Cheung K, Rashidi B, Yang X. Tumor suppressor LATS1 is a negative regulator of oncogene YAP. J Biol Chem. 2008; 283:5496–5509. [PubMed: 18158288]
19. Dong J, Feldmann G, Huang J, Wu S, Zhang N, Comerford SA, Gayyed MF, Anders RA, Maitra A, Pan D. Elucidation of a universal size-control mechanism in *Drosophila* and mammals. Cell. 2007; 130:1120–1133. [PubMed: 17889654]
20. Zhao B, Wei X, Li W, Udan RS, Yang Q, Kim J, Xie J, Ikenoue T, Yu J, Li L, Zheng P, Ye K, Chinnaiyan A, Halder G, Lai ZC, Guan KL. Inactivation of YAP oncoprotein by the Hippo pathway is involved in cell contact inhibition and tissue growth control. Genes Dev. 2007; 21:2747–2761. [PubMed: 17974916]
21. Lei QY, Zhang H, Zhao B, Zha ZY, Bai F, Pei XH, Zhao S, Xiong Y, Guan KL. TAZ promotes cell proliferation and epithelial-mesenchymal transition and is inhibited by the hippo pathway. Mol Cell Biol. 2008; 28:2426–2436. [PubMed: 18227151]
22. Oka T, Mazack V, Sudol M. Mst2 and Lats kinases regulate apoptotic function of Yes kinase-associated protein (YAP). J Biol Chem. 2008; 283:27534–27546. [PubMed: 18640976]
23. Fan Y, Mao R, Zhao Y, Yu Y, Sun W, Song P, Shi Z, Zhang D, Yvon E, Zhang H, Fu S, Yang J. Tumor necrosis factor-α induces RelA degradation via ubiquitination at lysine 195 to prevent excessive nuclear factor-κB activation. J Biol Chem. 2009; 284:29290–29297. [PubMed: 19706600]
24. Wu S, Liu Y, Zheng Y, Dong J, Pan D. The TEAD/TEF family protein Scalloped mediates transcriptional output of the Hippo growth-regulatory pathway. Dev Cell. 2008; 14:388–398. [PubMed: 18258486]
25. Ota M, Sasaki H. Mammalian Tead proteins regulate cell proliferation and contact inhibition as transcriptional mediators of Hippo signaling. Development. 2008; 135:4059–4069. [PubMed: 19004856]
26. Zhao B, Kim J, Ye X, Lai ZC, Guan KL. Both TEAD-binding and WW domains are required for the growth stimulation and oncogenic transformation activity of Yes-associated protein. Cancer Res. 2009; 69:1089–1098. [PubMed: 19141641]
27. Zhang H, Liu CY, Zha ZY, Zhao B, Yao J, Zhao S, Xiong Y, Lei QY, Guan KL. TEAD transcription factors mediate the function of TAZ in cell growth and epithelial-mesenchymal transition. J Biol Chem. 2009; 284:13355–13362. [PubMed: 19324877]
28. Lian I, Kim J, Okazawa H, Zhao J, Zhao B, Yu J, Chinnaiyan A, Israel MA, Goldstein LS, Abujarour R, Ding S, Guan KL. The role of YAP transcription coactivator in regulating stem cell self-renewal and differentiation. Genes Dev. 2010; 24:1106–1118. [PubMed: 20516196]
29. Cordenonsi M, Zanconato F, Azzolin L, Forcato M, Rosato A, Frasson C, Inui M, Montagner M, Parenti AR, Poletti A, Daidone MG, Dupont S, Basso G, Bicciato S, Piccolo S. The Hippo transducer TAZ confers cancer stem cell-related traits on breast cancer cells. Cell. 2011; 147:759–772. [PubMed: 22078877]
30. Wang K, Degerny C, Xu M, Yang XJ. YAP, TAZ, and Yorkie: A conserved family of signal-responsive transcriptional coregulators in animal development and human disease. Biochem Cell Biol. 2009; 87:77–91. [PubMed: 19234525]
31. Zhao B, Ye X, Yu J, Li L, Li W, Li S, Yu J, Lin JD, Wang CY, Chinnaiyan AM, Lai ZC, Guan KL. TEAD mediates YAP-dependent gene induction and growth control. Genes Dev. 2008; 22:1962–1971. [PubMed: 18579750]

32. Liu CY, Zha ZY, Zhou X, Zhang H, Huang W, Zhao D, Li T, Chan SW, Lim CJ, Hong W, Zhao S, Xiong Y, Lei QY, Guan KL. The hippo tumor pathway promotes TAZ degradation by phosphorylating a phosphodegron and recruiting the SCFβ-TrCP E3 ligase. J Biol Chem. 2010; 285:37159–37169. [PubMed: 20858893]
33. Park HW, Guan KL. Regulation of the Hippo pathway and implications for anticancer drug development. Trends Pharmacol Sci. 2013; 34:581–589. [PubMed: 24051213]
34. Varelas X, Sakuma R, Samavarchi-Tehrani P, Peerani R, Rao BM, Dembowy J, Yaffe MB, Zandstra PW, Wrana JL. TAZ controls Smad nucleocytoplasmic shuttling and regulates human embryonic stem-cell self-renewal. Nat Cell Biol. 2008; 10:837–848. [PubMed: 18568018]
35. Varelas X, Samavarchi-Tehrani P, Narimatsu M, Weiss A, Cockburn K, Larsen BG, Rossant J, Wrana JL. The Crumbs complex couples cell density sensing to Hippodependent control of the TGF-β-SMAD pathway. Dev Cell. 2010; 19:831–844. [PubMed: 21145499]
36. Sun Y, Yong KM, Villa-Diaz LG, Zhang X, Chen W, Philson R, Weng S, Xu H, Krebsbach PH, Fu J. Hippo/YAP-mediated rigidity-dependent motor neuron differentiation of human pluripotent stem cells. Nat Mater. 2014; 13:599–604. [PubMed: 24728461]
37. Song H, Mak KK, Topol L, Yun K, Hu J, Garrett L, Chen Y, Park O, Chang J, Simpson RM, Wang CY, Gao B, Jiang J, Yang Y. Mammalian Mst1 and Mst2 kinases play essential roles in organ size control and tumor suppression. Proc Natl Acad Sci USA. 2010; 107:1431–1436. [PubMed: 20080598]
38. Lee KP, Lee JH, Kim TS, Kim TH, Park HD, Byun JS, Kim MC, Jeong WI, Calvisi DF, Kim JM, Lim DS. The Hippo-Salvador pathway restrains hepatic oval cell proliferation, liver size, and liver tumorigenesis. Proc Natl Acad Sci USA. 2010; 107:8248–8253. [PubMed: 20404163]
39. McClatchey AI, Saotome I, Mercer K, Crowley D, Gusella JF, Bronson RT, Jacks T. Mice heterozygous for a mutation at the *Nf2* tumor suppressor locus develop a range of highly metastatic tumors. Genes Dev. 1998; 12:1121–1133. [PubMed: 9553042]
40. Lai ZC, Wei X, Shimizu T, Ramos E, Rohrbaugh M, Nikolaidis N, Ho LL, Li Y. Control of cell proliferation and apoptosis by Mob as tumor suppressor, mats. Cell. 2005; 120:675–685. [PubMed: 15766530]
41. Tapon N, Harvey KF, Bell DW, Wahrer DC, Schiripo TA, Haber D, Hariharan IK. *salvador* promotes both cell cycle exit and apoptosis in *Drosophila* and is mutated in human cancer cell lines. Cell. 2002; 110:467–478. [PubMed: 12202036]
42. Seidel C, Schagdarsurengin U, Blumke K, Wurl P, Pfeifer GP, Hauptmann S, Taubert H, Dammann R. Frequent hypermethylation of MST1 and MST2 in soft tissue sarcoma. Mol Carcinog. 2007; 46:865–871. [PubMed: 17538946]
43. Zhao B, Li L, Wang L, Wang CY, Yu J, Guan KL. Cell detachment activates the Hippo pathway via cytoskeleton reorganization to induce anoikis. Genes Dev. 2012; 26:54–68. [PubMed: 22215811]
44. Jimenez-Velasco A, Roman-Gomez J, Agirre X, Barrios M, Navarro G, Vazquez I, Prosper F, Torres A, Heiniger A. Downregulation of the large tumor suppressor 2 (*LATS2/KPM*) gene is associated with poor prognosis in acute lymphoblastic leukemia. Leukemia. 2005; 19:2347–2350. [PubMed: 16208412]
45. Harvey KF, Zhang X, Thomas DM. The Hippo pathway and human cancer. Nat Rev Cancer. 2013; 13:246–257. [PubMed: 23467301]
46. Chan SW, Lim CJ, Guo K, Ng CP, Lee I, Hunziker W, Zeng Q, Hong W. A role for TAZ in migration, invasion, and tumorigenesis of breast cancer cells. Cancer Res. 2008; 68:2592–2598. [PubMed: 18413727]
47. Hergovich A, Hemmings BA. Mammalian NDR/LATS protein kinases in hippo tumor suppressor signaling. Biofactors. 2009; 35:338–345. [PubMed: 19484742]
48. Lai D, Ho KC, Hao Y, Yang X. Taxol resistance in breast cancer cells is mediated by the hippo pathway component TAZ and its downstream transcriptional targets Cyr61 and CTGF. Cancer Res. 2011; 71:2728–2738. [PubMed: 21349946]
49. Overholtzer M, Zhang J, Smolen GA, Muir B, Li W, Sgroi DC, Deng CX, Brugge JS, Haber DA. Transforming properties of YAP, a candidate oncogene on the chromosome 11q22 amplicon. Proc Natl Acad Sci USA. 2006; 103:12405–12410. [PubMed: 16894141]

50. Zhao B, Tumaneng K, Guan KL. The Hippo pathway in organ size control, tissue regeneration and stem cell self-renewal. Nat Cell Biol. 2011; 13:877–883. [PubMed: 21808241]
51. Nomura T, Khan MM, Kaul SC, Dong HD, Wadhwa R, Colmenares C, Kohno I, Ishii S. Ski is a component of the histone deacetylase complex required for transcriptional repression by Mad and thyroid hormone receptor. Genes Dev. 1999; 13:412–423. [PubMed: 10049357]
52. Deheuninck J, Luo K. Ski and SnoN, potent negative regulators of TGF-β signaling. Cell Res. 2009; 19:47–57. [PubMed: 19114989]
53. He J, Tegen SB, Krawitz AR, Martin GS, Luo K. The transforming activity of Ski and SnoN is dependent on their ability to repress the activity of Smad proteins. J Biol Chem. 2003; 278:30540–30547. [PubMed: 12764135]
54. Lamouille S, Xu J, Derynck R. Molecular mechanisms of epithelial–mesenchymal transition. Nat Rev Mol Cell Biol. 2014; 15:178–196. [PubMed: 24556840]
55. Zhu Q, Krakowski AR, Dunham EE, Wang L, Bandyopadhyay A, Berdeaux R, Martin GS, Sun L, Luo K. Dual role of SnoN in mammalian tumorigenesis. Mol Cell Biol. 2007; 27:324–339. [PubMed: 17074815]
56. Azzolin L, Zanconato F, Bresolin S, Forcato M, Basso G, Bicciato S, Cordenonsi M, Piccolo S. Role of TAZ as mediator of Wnt signaling. Cell. 2012; 151:1443–1456. [PubMed: 23245942]
57. Adler JJ, Heller BL, Bringman LR, Ranahan WP, Cocklin RR, Goebl MG, Oh M, Lim HS, Ingham RJ, Wells CD. Amot130 adapts atrophin-1 interacting protein 4 to inhibit Yes-associated protein signaling and cell growth. J Biol Chem. 2013; 288:15181–15193. [PubMed: 23564455]
58. Jahchan NS, Wang D, Bissell MJ, Luo K. SnoN regulates mammary gland alveologenesis and onset of lactation by promoting prolactin/Stat5 signaling. Development. 2012; 139:3147–3156. [PubMed: 22833129]
59. Stroschein SL, Wang W, Zhou S, Zhou Q, Luo K. Negative feedback regulation of TGF-β signaling by the SnoN oncoprotein. Science. 1999; 286:771–774. [PubMed: 10531062]
60. Ji X, Lu H, Zhou Q, Luo K. LARP7 suppresses P-TEFb activity to inhibit breast cancer progression and metastasis. eLife. 2014; 3:e02907. [PubMed: 25053741]

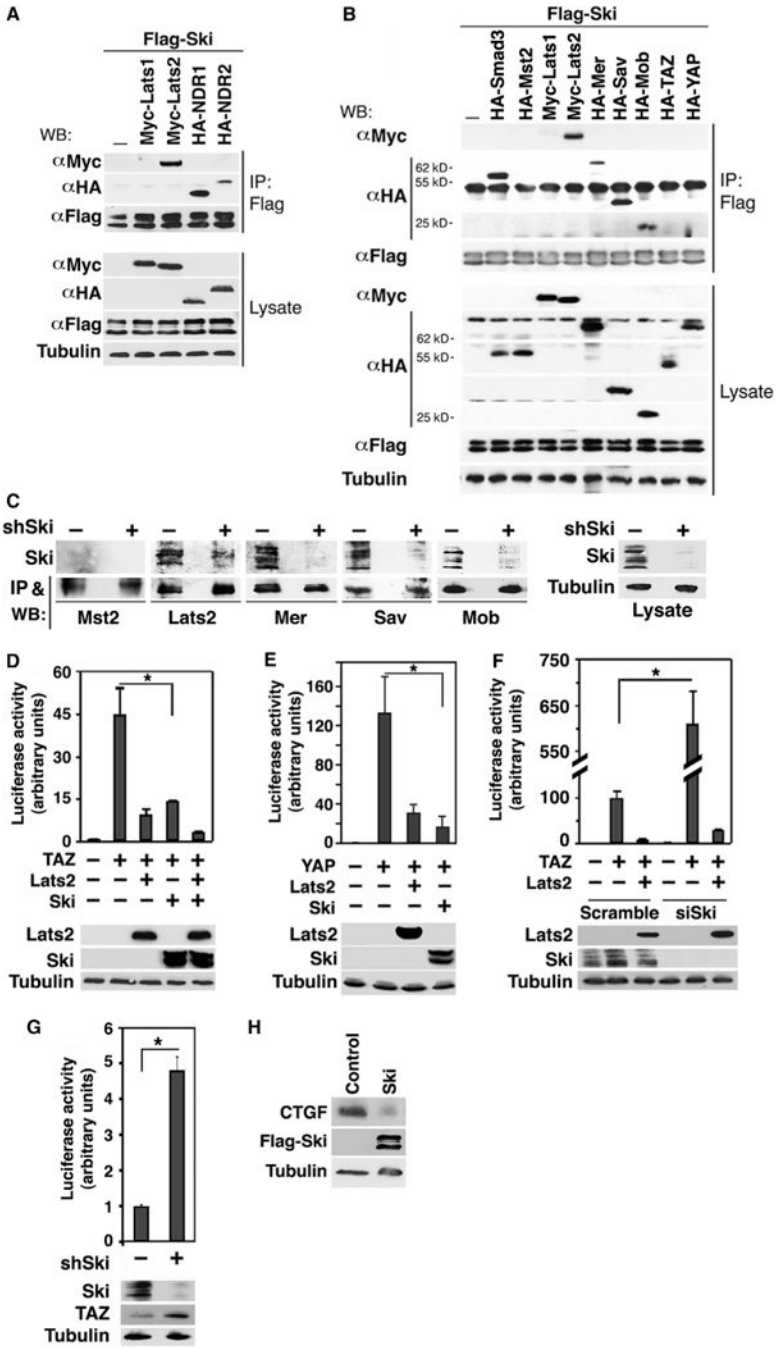

Fig. 1. Ski interacts with multiple components of the Hippo pathway and inhibits the transcriptional activity of TAZ and YAP

(**A**) Lysates from 293T cells expressing Flag-Ski together with control vector, Myc-Lats1, Myc-Lats2, HA-NDR1, or HA-NDR2 were subjected to immunoprecipitation (IP) with anti-Flag beads, and proteins associated with Flag-Ski were detected by Western blotting (WB) with anti-Myc or anti-HA antibodies (upper panel). The abundance of these proteins in the lysates was examined by Western blotting (lower panel). (**B**) Myc-or HA-tagged Hippo signaling proteins associated with Ski were isolated by immunoprecipitation with anti-Flag

beads and detected by Western blotting with anti-Myc or anti-HA antibodies. Smad3 was used as a positive control for binding to Ski. Tubulin was used as a loading control. (**C**) Interactions between endogenous Ski and various Hippo signaling proteins were examined in MDA-MB-231 cells transfected or not with Ski shRNA (shSki) by immunoprecipitation with antibodies against Mst2, Lats2, Mer, Sav, and Mob followed by Western blotting with anti-Ski (upper panels). The abundance of Mst2, Lats2, Mer, Sav, and Mob in the immunoprecipitates was assessed by Western blotting with the corresponding antibodies (lower panels). The knockdown of Ski was evaluated by Western blotting with anti-Ski antibody in cell lysates (right panel). (**D** and **E**) Luciferase activity was measured in human embryonic kidney (HEK) 293 cells expressing HA-TAZ (D) or HA-YAP (E) in the presence or absence of HA-Lats2 or Flag-Ski. (**F**) Reducing endogenous Ski by siRNA increases the transcriptional activity of TAZ. (**G**) Reducing endogenous Ski by shRNA enhanced the transcriptional activity of endogenous TAZ in MDA-MB-231 cells. (**H**) Ski decreases the abundance of endogenous CTGF. CTGF and Ski abundance in MCF10A control or Ski-overexpressing cells was examined by Western blotting. Tubulin was used as a loading control. Data in the graphs in (D) to (G) were derived from at least three independent experiments and are presented as means ± SEM (Student's *t* test, $*P < 0.05$). Western blots in (A) to (C) and (H) are representative of three independent experiments.

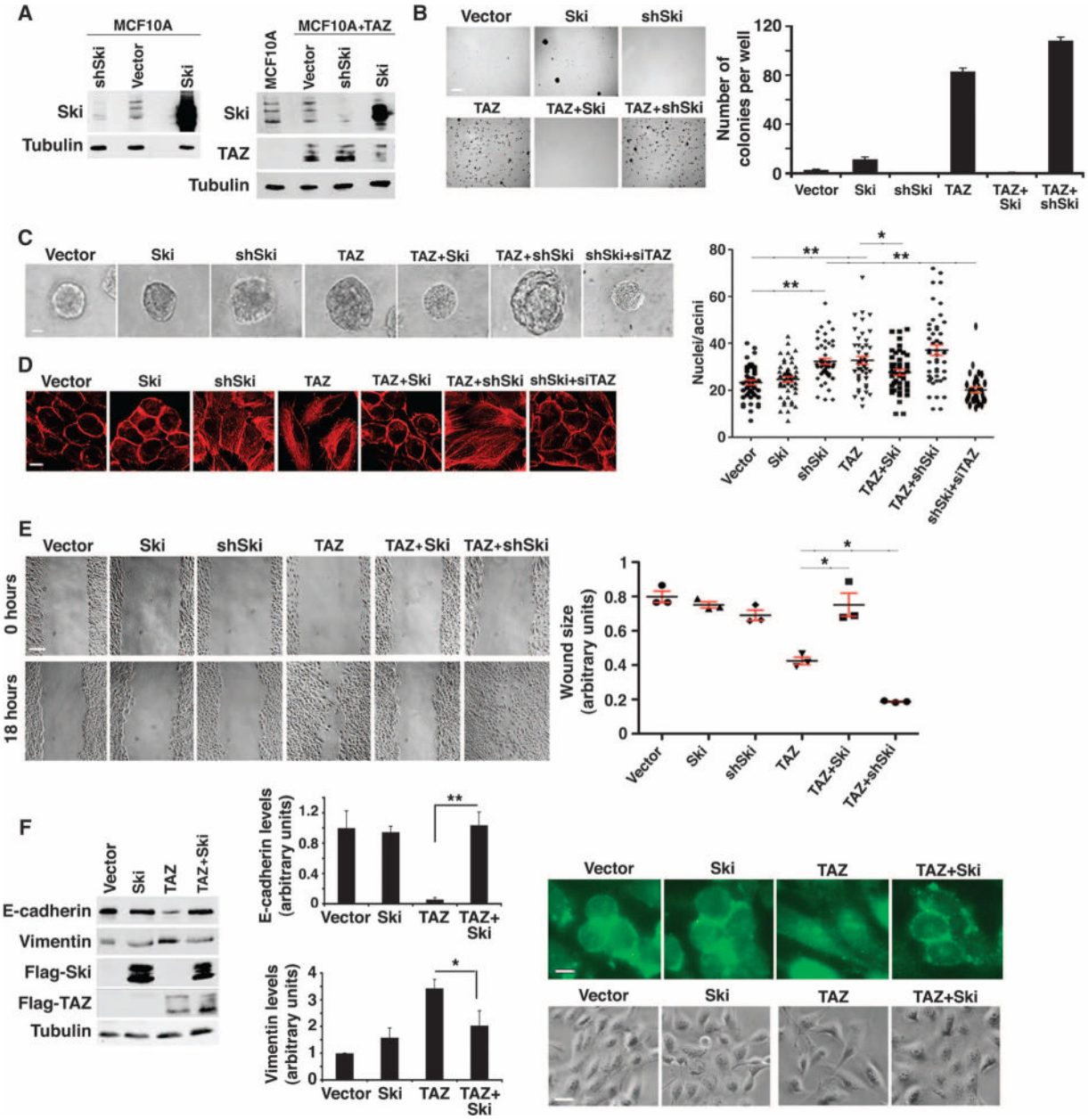

Fig. 2. Ski reverses TAZ-induced oncogenic transformation and EMT

(**A**) Western blot analysis of Ski and TAZ abundance in MCF10A or MCF10A/TAZ cells stably infected with Ski cDNA or shSki. Western blots are representative of two independent experiments. (B) Ski blocked anchorage-independent growth induced by TAZ. Soft agar colonies formed by MCF10A cells stably expressing various cDNAs and shRNAs as indicated were stained and quantified. Data in the graph were derived from at least three independent experiments and are presented as means ± SEM [Student's *t* test, *P < 0.05 (P value was calculated after colony counts were averaged and converted to logarithmic scale)]. Scale bar, 3 mm. (C) Phase-contrast images of 3D acini formed by MCF10A cells stably expressing various constructs as indicated. The size of an acinus was determined by the number of nuclei in each acinus. Forty acini from three independent experiments were

quantified for each cell line and presented in the graph as means ± SEM [analysis of variance (ANOVA), Newman-Keuls multiple comparison test; *P < 0.05, **P < 0.01]. Scale bar, 40 μm. Significant differences between the control and shSki or TAZ cells and between shSki and shSki + TAZ siRNA (siTAZ) cells (**P<0.01) and between TAZ and Ski-TAZ cells (*P< 0.05) were detected. (D) Actin stress fiber formation was visualized by staining with rhodamine-conjugated phalloidin. Images are representative of three independent experiments. Scale bar, 20 μm. (E) Wound healing assay. Data in the graph were derived from at least three independent experiments and are presented as means ± SEM (ANOVA, Newman-Keuls multiple comparison test; *P < 0.05). Scale bar, 300 μm. (F) Ski reversed the effect of TAZ on the abundance of E-cadherin and vimentin as determined by Western blotting. Data in the graph were derived from at least three independent experiments and are presented as means ± SEM (Student's t test, *P < 0.05 and **P < 0.01). The cell morphology (scale bar, 50 μm) and E-cadherin localization (scale bar, 20 μm) are shown in the panels to the right. Images are representative of three independent experiments.

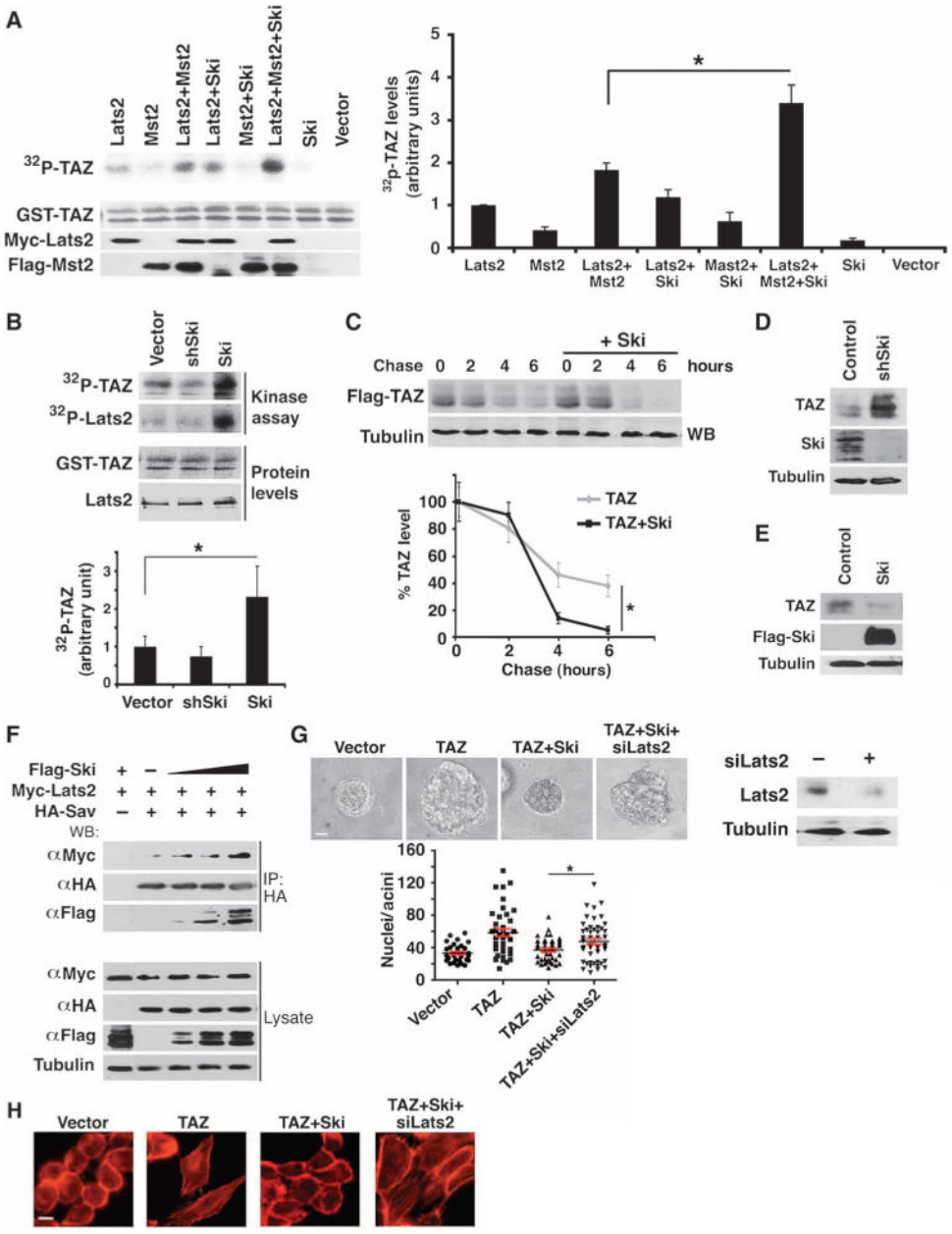

Fig. 3. Ski enhances phosphorylation of TAZ by Lats2

(**A**) Ski enhanced the kinase activity of Lats2. Myc-Lats2 was immunoprecipitated from 293T cells expressing Myc-Lats2 alone or together with Mst2 and Ski as indicated and subjected to in vitro kinase assay using GST-TAZ as a substrate. The abundance of GST-TAZ, Myc-Lats2, and Flag-Mst2 was measured by Western blotting (lower panels). Western blots are representative of three independent experiments. ^{32}P-TAZ abundance was quantified from at least three independent experiments, and data are presented as means ± SEM (Student's *t* test, **P* < 0.05). (**B**) Endogenous Lats2 was immunoprecipitated from MCF10A cells stably expressing control vector, Ski, and shSki and subjected to an in vitro kinase assay with GST-TAZ as an exogenous substrate. The abundance of GST-TAZ and Lats2 was measured by Western blotting. Western blots are representative of three

independent experiments. Data are presented as means ± SEM (Student's *t* test, **P* < 0.05). (**C**) Pulse-chase assays. ^{35}S-labeled Flag-TAZ was immunoprecipitated with anti-Flag beads and detected by autoradiography. Data in the graph were derived from at least three independent experiments and are presented as means ± SEM (Student's *t* test, **P* < 0.05). (**D** and **E**) Western blot analysis indicated that endogenous TAZ abundance was enhanced in shSki-expressing cells (D) and reduced in Ski over-expressing cells (E). Western blots are representative of three independent experiments. (**F**) Ski enhanced the Lats2-Sav interaction. HA-Sav was immunoprecipitated from cells transfected with fixed amounts of Myc-Lats2 and HA-Sav and increasing amounts of Flag-Ski, and the associated Myc-Lats2 was detected by Western blotting with anti-Myc antibody. Cells transfected with Flag-Ski and Myc-Lats2 were used as negative controls for anti-Myc immunoprecipitation. Western blots are representative of three independent experiments. (**G**) Reducing Lats2 by siRNA reversed the inhibition of TAZ by Ski in 3D morphogenesis. Top: Phase-contrast images of 3D acini. Bottom: Forty acini from three independent experiments were quantified for each cell line and presented in the graph as means ± SEM (ANOVA, Newman-Keuls multiple comparison test). Significant differences between TAZ+Ski cells expressing control vector and Lats2 siRNA (siLats2) were detected (***P* < 0.05). Scale bar, 40 μm. (**H**) Reducing Lats2 reversed the Ski inhibition of TAZ-dependent actin stress fiber formation. Images are representative of three independent experiments. Scale bar, 20 μm.

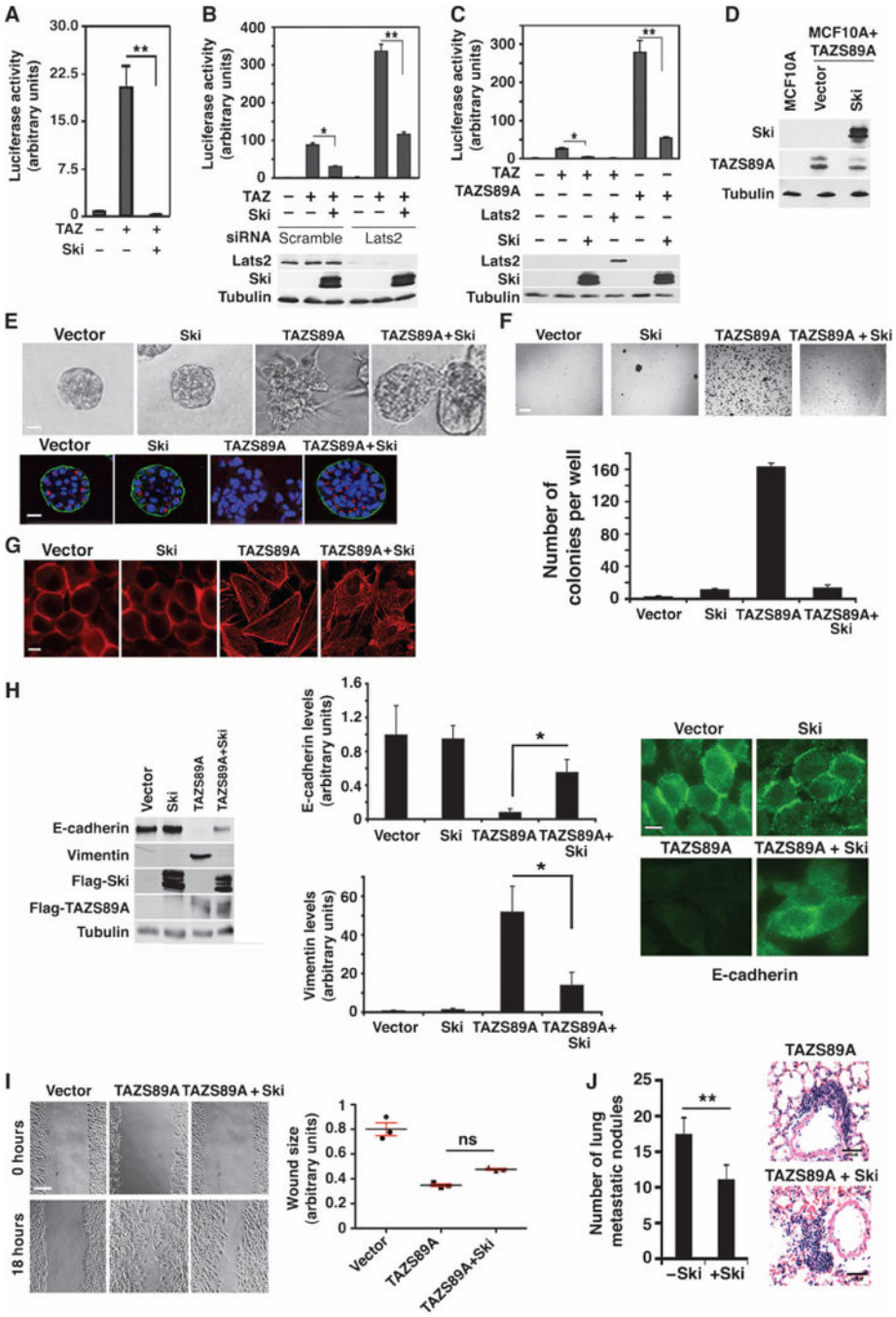

Fig. 4. Ski also inhibits TAZ through a Lats2-independent mechanism

(**A**) Ski inhibited TAZ transcription activity in $Sav^{-/-}$ ACHN cells as measured by a luciferase assay. (**B**) Ski could inhibit TAZ independently of Lats2. Luciferase activity was measured in HEK293 cells that were transfected with Lats2 siRNA before being transfected with HA-TAZ, Flag-Ski, and a luciferase reporter. (**C**) Ski inhibited the transcriptional activity of TAZS89A in a luciferase assay. WT TAZ with Lats2 or Ski was used as a positive control. Data in the graphs in (A) to (C) were derived from at least three independent experiments and are presented as means ± SEM (Student's *t* test, $*P < 0.05$,

$P < 0.01$). (D**) The abundance of Ski and TAZS89A in MCF10A cells stably expressing TAZS89A with or without Ski was measured by Western blotting. Western blots are representative of two independent experiments. (**E**) Ski reversed transformation induced by TAZS89A. Top: Phase-contrast images of acini cultured in 3D Matrigel. Bottom: Confocal images of acini stained for α_6-integrin (green) and Golgi matrix protein of 130 kD (GM130; red). Nuclei are stained with 4′,6-diamidino-2-phenylindole (blue). Images are representative of three independent experiments. Scale bar, 40 μm. (**F**) Ski inhibited anchorage-independent growth induced by TAZ-S89A. Soft agar colonies formed by MCF10A/TAZS89A cells with or without Ski were stained with 3-(4,5-dimethylthiazol-2-yl)-2,5-diphenyltetrazolium bromide (MTT) and quantified. Data in the graph were derived from at least three independent experiments and are presented as means ± SEM [Student's *t* test, *P < 0.05 (*P* value was calculated after colony counts were averaged and converted to logarithmic scale)]. Scale bar, 3 mm. (**G**) Actin stress fiber formation was analyzed by staining with rhodamine-conjugated phalloidin. Images are representative of three independent experiments. Scale bar, 20 μm. (**H**) Ski reversed the effects of TAZS89A on E-cadherin (partially) and vimentin abundance as shown by Western blotting (left) and immunofluorescence staining (right). Data shown in the graphs (middle) were derived from at least three independent experiments and are presented as means ± SEM (Student's *t* test, *$P < 0.05$). Scale bar, 20 μm. (**I**) Wound healing assay. Ski partially reversed the increase in cell motility caused by TAZS89A. Data in the graph were derived from at least three independent experiments and are presented as means ± SEM (ANOVA, Newman-Keuls multiple comparison test). ns, nonsignificant differences. (**J**) Ski reduced the metastatic potential of TAZ in vivo. Representative images of the metastatic nodules in hematoxylin and eosin (H&E)–stained lung sections from mice injected with cells expressing TAZS89A or Ski+TAZS89A are shown on the right. Scale bar, 100 μm. Quantification of the number of metastatic nodules from three sections per mouse and six mice per cell line is shown in the bar graph on the left. Data are presented as means ± SEM (Student's *t* test, *$P = 0.004$).

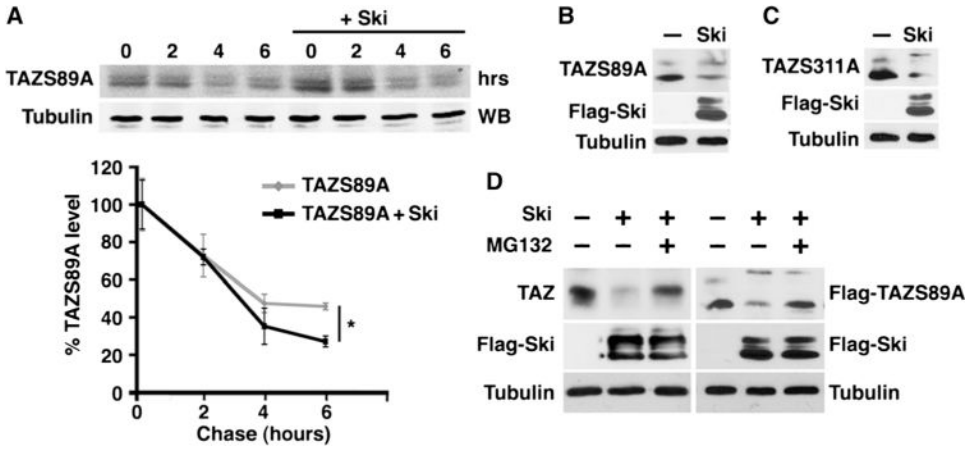

Fig. 5. Ski also destabilizes TAZ through a Lats2-independent mechanism

(**A**) Ski decreased the stability of TAZS89A. Cells transfected with Flag-TAZS89A together with or without Flag-Ski were subjected to a pulse-chase assay. Data in the graph were derived from at least three independent experiments and are presented as means ± SEM (Student's *t* test, **P* < 0.05). (**B** and **C**) Western blotting analysis shows that overexpression of Ski decreased the abundance of TAZS89A (B) and TAZS311A (C). Western blots are representative of two independent experiments. (**D**) Suppression of TAZ and TAZS89A by Ski required the proteasome. The abundance of endogenous TAZ (left) or TAZS89A (right) was measured in MG132-treated cells expressing Flag-Ski alone (left) or Flag-Ski plus TAZS89A (right) by Western blotting. Western blots are representative of three independent experiments.

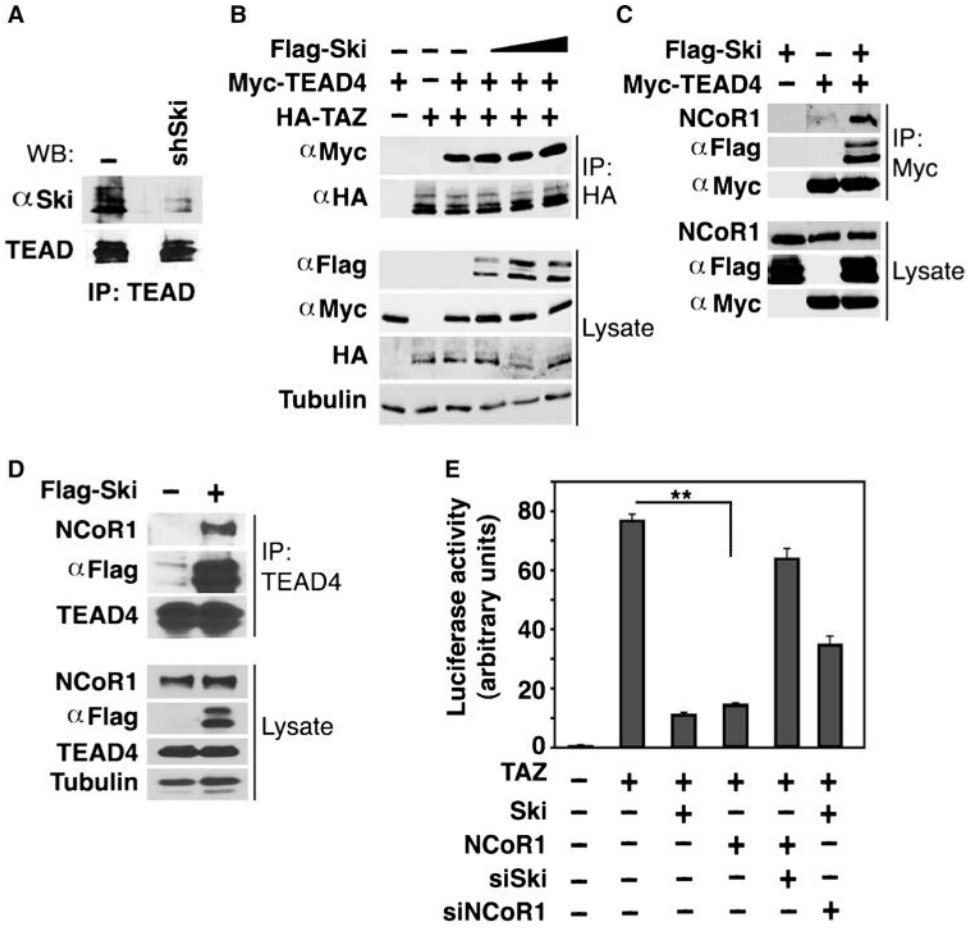

Fig. 6. Ski recruits NCoR1 to the TEAD/TAZ complex

(**A**) Ski bound to TEAD. Endogenous Ski was immunoprecipitated from control or shSki-expressing MDA-MB-231 cells with anti-Ski, and associated endogenous TEAD was detected by Western blotting with an anti-TEAD antibody that cross-reacts with multiple TEAD isoforms. Western blots are representative of two independent experiments. (**B**) Ski did not affect the TAZ-TEAD interaction. 293T cells expressing fixed amounts of HA-TAZ and Myc-TEAD4 and increasing amounts of Flag-Ski were pretreated with MG132 before being subjected to anti-HA immunoprecipitation followed by Western blotting with anti-Myc. Western blots are representative of two independent experiments. (**C**) TEAD formed a complex with NCoR1 in the presence of Ski. 293T cells were transfected with Myc-TEAD4 alone, Flag-Ski alone, or the two together. TEAD4 was immunoprecipitated with anti-Myc, and associated endogenous NCoR1 was detected by Western blotting with anti-NCoR1. Western blots are representative of two independent experiments. (**D**) Endogenous TEAD and NCoR1 formed a complex in the presence of Ski. TEAD4 was immunoprecipitated from MCF10A/Ski cells with anti-TEAD, and associated endogenous NCoR1 was detected by Western blotting with anti-NCoR1. Western blots are representative of two independent experiments. (**E**) Luciferase activity was measured in HEK293T cells expressing HA-TAZ together with various cDNA and siRNA constructs as indicated. siNCoR1, NCoR1 siRNA.

Data in the graph were derived from at least three independent experiments and are presented as mean ± SEM (Student's *t* test, $^{**}P < 0.01$).